

- Requested start date: February 1st, 2024, requested proposal duration: 5 years
- Related Letter of Intent (LOI): None
- Related preliminary proposal: None
- Prime organization: Whittier College
- Primary place of performance:
 - Organization name: Whittier College
 - Country: United States of America
 - Street address: 3406 E. Philadelphia Street
 - City: Whittier
 - State: California
 - ZIP Code: 90602
- Other federal agencies: None
- Other information: Antarctic fieldwork

CAREER: Translation, Acceleration, and Diversification of Science and Engineering with Open-Source Computational Electromagnetism and Additive Manufacturing

Radio-frequency (RF) phased-array systems optimized with machine learning have become powerful tools in science and engineering. Recent progress in phased-array radar development has applications in particle astrophysics [1–4], polar research [5, 6], and 5G mobile communications [7]. Phased-arrays are comprised of RF antennas working in tandem to boost received signal sensitivity, and to actively scan transmitted signals without moving parts. Two pathways for progress in phased array design and production that will enhance future scientific work are cost reduction and the introduction of open-source software. The electromagnetic properties of phased arrays are designed with expensive, proprietary software that does not interface with open-source machine learning tools [8]. Phased arrays are then manufactured using costly and time-consuming traditional machining techniques. Ongoing scientific and engineering efforts can be enhanced by a solution that allows machine learning optimization to flourish, reduces design and manufacturing costs, and diversifies participation by reducing financial barriers. Undergraduate STEM education will be enhanced with CEM, machine learning, and 3D printing, as research and educational opportunities can be integrated the STEM curriculum.

We propose to create the first open-source CEM and additive manufacturing ecosystem capable of 3D-printing phased arrays with conductive filament [8–10]. We have already shown that open-source CEM tools used in photonics can drive the RF phased-array design process [3, 11, 12]. This research will support diverse projects like IceCube Gen2 (radio), Center for Remote Sensing and Systems (CReSIS) missions, and Office of Naval Research (ONR) radar projects. One application in particle astrophysics is the Askaryan Radio Array (ARA), in which phased arrays have increased sensitivity to ultra high-energy neutrino (UHE- ν) interactions in the ice sheet beneath the South Pole [13]. The arrays are vertically polarized, due to mechanical constraints within the ice. By combining machine learning with CEM, we seek a *horizontally polarized* design that overcomes these mechanical constraints, boosting the chances of making the first UHE- ν observations in history [14]. This research will *accelerate* and *diversify* research in UHE- ν , climate science, and RF engineering by *translating* successes in CEM and materials research. This work will be integrated into our curriculum and research programming at Whittier College, a Title-V Hispanic Serving Institution (HSI).

This work will provide research and educational opportunities to diverse undergraduates at Whittier College. We have a proud tradition of providing access to higher education to Spanish-speaking and historically marginalized students, and we are the only HSI member of the IceCube Gen2 collaboration. People of color and first-generation students make up 63% and 29% of our student body, respectively. Internal assessment studies indicate that students of color receive lower grades than their peers in introductory STEM courses. We have learned from workshops hosted by the Cottrell Scholars Network that emphasizing the dignity and self-efficacy of diverse students can increase their performance [15, 16]. Emphasis in these areas makes students feel they *belong* in our courses, despite encountering adversity. In keeping with the theme of *translation*, and in order to emphasize the dignity of our students no matter their background, we seek to create a bilingual (Spanish and English) mobile application (app) that introduces STEM concepts within a welcoming digital environment.

There is precedent for learning apps enhanced by machine learning in the Duolingo method for language and mathematics [17]. We seek to provide data insights about student learning to instructors through the app, which will lead to more efficient and customized classroom instruction. A prototype application is being built by Whittier College undergraduates. The creation and implementation of this program represents an opportunity for Whittier College students to enhance the learning experience for their peers while gaining valuable coding and machine learning experience. In addition to algorithms presented within the Duolingo method, the educational data mining (EDM) literature provides examples of apps that boost engagement and success in introductory STEM courses [18–21]. Members of our community have shared that translating mathematics and physics exercises into Spanish aids in solving them. Our application will boost their skills and build confidence by offering them engaging, game-like physics training in the language of their choice. Finally, we propose to create a bilingual lecture series and recruitment events designed to welcome the broader community into the Whittier College environment.

CAREER: Translation, Acceleration, and Diversification of Science and Engineering with Open-Source Computational Electromagnetism and Additive Manufacturing

Jordan C Hanson, PhD
Assistant Professor of Physics and Astronomy
Whittier College
Whittier, CA

June 12, 2023

Contents

1 Project Description	3
1.1 Computational Electromagnetism and Additive Manufacturing	4
1.1.1 RF Laboratory Capability and Prior ONR Funding	7
1.2 The Connection to Ultra-High Energy Neutrino Observations	8
1.3 The Connection to Remote Sensing of Ice Sheets	9
1.4 Integration of Research and Education at Whittier College	11
1.4.1 Course Integrations - Electromagnetism and Computational Physics	11
1.4.2 Course Integrations - Computer Logic and Digital Circuit Design, and Digital Signal Processing	13
1.4.3 Course Integrations - Introduction to Data Science with Python, and Machine Learning	13
1.5 Translation of STEM Research for our Community	14
1.6 Bilingual Public Lectures and Recruitment Events	15
1.7 Timeline and Project Planning	15

Project Description

Radio-frequency (RF) phased arrays have applications in radar telemetry, telecommunications, ground-penetrating radar, scientific instrumentation, and remote sensing [1, 2, 5, 13, 22–24]. In the one-dimensional case, N three-dimensional RF antennas are arranged in a line with fixed spacing. In the two-dimensional case, $N \times M$ three-dimensional antenna elements are arranged in a two-dimensional grid with fixed spacing in both dimensions. The signal to noise ratio (SNR) of received signals in arrays of dimension N is boosted by a factor of $\approx \sqrt{N}$, because the N signals are combined coherently while thermal background noise adds like \sqrt{N} . The SNR boost is critical for certain kinds of scientific observations. For example, systems created at the Center for Remote Sensing and Integrated Systems (CReSIS) are flown in polar regions to perform radar sounding of ice sheets for the purposes of geophysics and climate science [5]. Reflected signals carry information about the ice depth, temperature, and internal structure of the ice. The radio echoes have small SNRs that require phased arrays.

Traditionally, RF phased arrays are designed with commercial computational electromagnetism (CEM) software. Radio antennas and phased arrays have *radiation patterns* that define directions of maximum transmission power and received sensitivity. Radiation patterns have a main lobe in which most of the radiation is concentrated, and the angular width of the main lobe is called the beam width. Other parameters like S-parameters quantify the efficiency of the systems. CEM packages like XFDTD and HFSS are used to model these properties as a function of frequency [25, 26]. The XFDTD package, for example, relies on the finite difference time domain (FDTD) method. The FDTD approach is a CEM technique in which spacetime and Maxwell's equations are broken into discrete form. Depending on the software license and version, the current price of these products ranges between \$5,000 and \$40,000 USD. These costs are prohibitive for HSI undergraduate institutions like Whittier College. Removing this financial barrier to entry would allow diverse undergraduates to study professional RF design.

Another drawback of commercial CEM software is the lack of source code access impedes the incorporation of modern machine learning packages. Phased array properties are determined by the shape of the RF elements and the grid properties of the array. The parameter space is driven by the complex variety of RF element shapes. When combined with open-source CEM software, modern machine learning algorithms can locate optimal solutions. The authors of [8] review a number of open-source CEM packages. One interesting choice they describe is the MIT Electromagnetic Equation Propagation (MEEP) package [12]. Though MEEP was designed for μm wavelengths in photonics applications, we have shown that the scale-invariance of Maxwell's equations allows MEEP users to translate designs to wavelengths at the cm-scale. We have also shown that MEEP can drive the RF phased-array design loop, and that 3D printer schematics can be extracted from this process [3, 11, 12]. Through this project, diverse undergraduates will gain experience translating machine learning results into a practical solution.

Filament for 3D printers that is conductive in the RF bandwidth is now available commercially. Funded through an NSF Translational Impact (TI) award (1721644), Multi3D LLC. has produced filament with a resistivity of just $10^{-2}\Omega\text{ cm}$: the Electrifi filament. Several antenna designs have already been produced [10, 27]. These examples include horn antennas with gain factors of 15 dB at 5.8 GHz, and microstrip patch antennas with gains of 1-2 dB at 2.5 GHz. The results match expectations from commercial CEM software. There are, however, virtually no examples of 3D printed RF phased arrays in

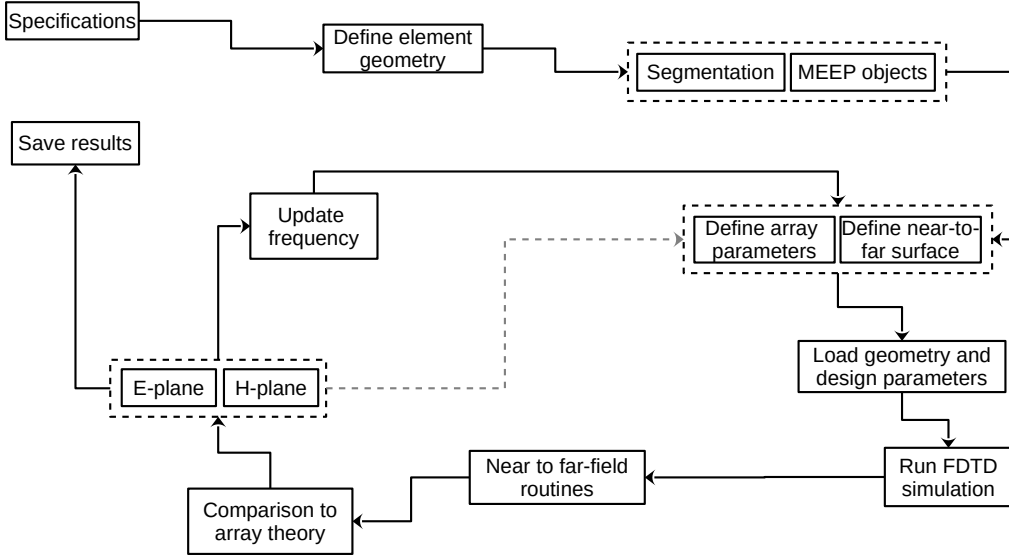


Figure 1.1: Our design process for RF phased arrays from [3], adapted from Fig. 1 of the review [8].

the [0.1 - 1] GHz bandwidth. This bandwidth is the most relevant for the aforementioned applications in particle astrophysics and geophysics. Further, whole new designs can be discovered that improve on designs like the horn and patch antennas by merging machine learning packages with MEEP. In Sec. 1.1, we review progress already made at Whittier College. In Sec. 1.2, we show how this work enhances the field of UHE- ν detection. In Sec. 1.3, we show how this work enhances the field of radio sounding of ice sheets and ice shelves. In Sec. 1.4, we articulate our vision for the integration of this research into our STEM curriculum. In Sec. 1.7, we provide a project timeline, broken into manageable phases. In Sec. 1.5, we describe the phase of this project designed to help us provide a better education to our students and broader community .

1.1 Computational Electromagnetism and Additive Manufacturing

In Summer 2020, we received a Faculty Fellowship from the Office of Naval Research (ONR) to design phased arrays in the [0.1 - 5] GHz bandwidth. This bandwidth is relevant for projects like IceCube Gen2 (radio)¹. Given our background in the use of RF detectors for UHE- ν observations in Antarctica (see Sec. 1.2), we were qualified to introduce RF phased arrays to our Navy colleagues. The audience included engineers and programmers that work in acquisition and development for the Naval Surface Warfare Center (NSWC), Corona Division (NSWC Corona). Our goal was to design a phased array to be integrated as a transmitter in an anechoic chamber that can mimic moving radar echoes. The facility will serve as a testing facility for active radar systems. We began by giving lectures on the electromagnetism of phased arrays, with scientific applications. Our design flow is depicted in Fig. 1.1. To minimize costs and increase undergraduate student access, we decided to investigate open-source CEM options for the design.

We encountered the aforementioned review article in the open-access journal *Electronics* that indicated there are open-source CEM tools that can be adapted to phased array analysis. Our design flow in Fig. 1.1 is adapted from Fig. 1 of the review to include specific tasks required for phased arrays, and algorithms for the computation of far-field radiation patterns. MEEP was noted by the authors in the review as the most advanced among open-source FDTD programs, but they did not benchmark it against HFSS or XFDTD due to the “steep” learning curve. In Summer 2020, we ascended the learning curve and adapted

¹Whittier College is a member institution of the IceCube Gen2 collaboration.

MEEP to RF systems. A key insight was that MEEP takes advantage of the *scale invariance* of Maxwell's Equations. The simplest way to understand this is to understand how MEEP uses relative units when discretizing Maxwell's equations for Python code.

Like other FDTD methods, MEEP uses a Yee lattice to discretize Maxwell's equations [28]. When the speed of light is set to unity ($c = 1$), distance and time units become the same. Frequency and wavelength units are the inverse of each other. But distance and wavelength can take *any* unit of length in the Yee lattice. Most MEEP users interpret this unit of length to be 1 μm for photonics applications. For example, a *relative* frequency (unit-less) of 0.5 corresponds to a *relative* wavelength of 2. When interpreted as 2 μm , the frequency is 150 THz in real units in the optical bandwidth. Interpreted as 2 cm, the real frequency is 15 GHz. A *relative* frequency of 0.05 corresponds to the RF frequency 1.5 GHz. Assuming design components have sufficient conductivity at RF frequencies, we have re-purposed MEEP as an RF simulator.

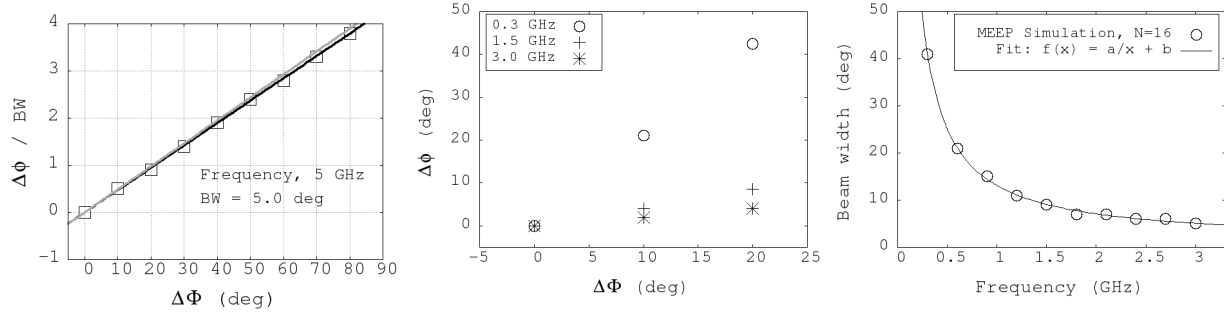


Figure 1.2: (Left) The beam angle $\Delta\phi$ divided by the beam width BW for the $N = 16$ one-dimensional Yagi array versus $\Delta\Phi$, the phase shift per element. The gray line represents theoretical expectation, and the black line is a linear fit to the data. (Middle) $\Delta\phi$ versus $\Delta\Phi$ for the $N = 16$ version of the one-dimensional horn array, for several frequencies. (Right) The dependence of the beam width on frequency for the one-dimensional $N = 16$ horn array. The black line is a functional fit to the data $f(x) = a/x+b$ with $a = 12.0 \pm 0.1$ degree GHz, and $b = 1.1 \pm 0.2$ degrees.

By Fall 2020, we were producing CEM models using MEEP that matched expected phased array properties. For a one-dimensional array with N elements, there is a linear relationship between the radiated plane-wave direction $\Delta\phi$, and the phase shift per element $\Delta\Phi$. The $\Delta\phi$ is also called the *beam angle*. Figure 1.2 contains results for our first phased array models in which the elements were Yagi-Uda antennas and horn antennas. The linear relationship between $\Delta\phi$ and $\Delta\Phi$ is evident in the data. The $\Delta\phi$ is divided by the beam width (BW) in Fig. 1.2 (left), and is left in degrees in Fig. 1.2 (middle). In Fig. 1.2 (left), the single-frequency $N = 16$ Yagi array can steer a 5 GHz plane wave up to four beam widths to the right or left of the forward direction. In Fig. 1.2 (middle), results are shown for an $N = 16$ array of horn antennas. Unlike the Yagi-Uda, the horns are broadband radiators. Thus, the linear relationship is shown for 0.3, 1.5, and 3.0 GHz. The beam width is not constant, so $\Delta\phi$ was left in degrees in Fig. 1.2 (middle). In Fig. 1.2 (right), the inverse relationship between beam width and frequency is shown.

We also produce CEM phased array radiation patterns that match array theory. The pattern of a phased array can be derived from first principles [3]. The *pattern multiplication theorem* states that the radiation pattern of a phased array of N identical elements will be that of a row of N point sources, multiplied by the radiation pattern of the element. In Fig. 1.3 (left and middle), the radiated E-field of a $N = 16$ horn array is shown in the E-plane (x-y plane). The radiation pattern is represented by the blue curve in Fig. 1.3 (right). The beam angle of the main lobe is $\Delta\phi = 9$ degrees above the x-axis, matching the theoretical expectation in red. The red curve corresponds to the formula for a row of N point sources, which has a back lobe at $\Delta\phi = 171$ degrees due to symmetry. The horn array has no back lobe because the individual horns suppress it, as expected from the pattern multiplication theorem. Like the theoretical expectation, the CEM pattern has *side lobes* around the main lobe (≈ -15 dB). We achieved similar results for two-dimensional arrays of Yagi-Uda and horns. Our revelation that MEEP could be used to design RF phased arrays earned the article Top 10 honors for December 2020 - May 2021 from the editors of *Electronics*.

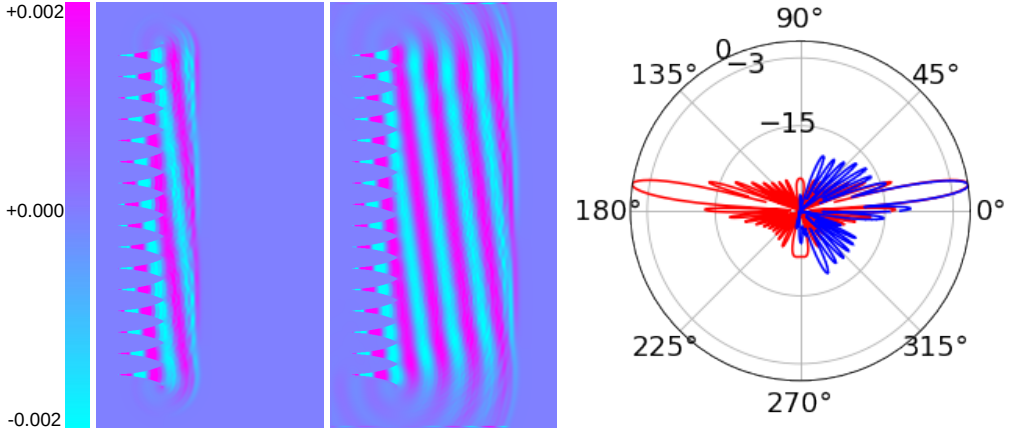


Figure 1.3: (Left) The $N = 16$ horn array, radiating the linearly polarized $\vec{E}(x, y, t)$ (y-component shown, in arbitrary units) at $t = 1$ ns into the simulation run, and (middle) at $t = 2$ ns into the run. The 2D area is $80 \times 150 \text{ cm}^2$. The frequency is 2.5 GHz, and the beam angle is $\Delta\phi = 9$ degrees above the x-axis. (Right) The normalized radiated power in dB versus $\Delta\phi$ in degrees. The blue curve represents the results from MEEP, and the red curve is the theoretical expectation from N point sources.

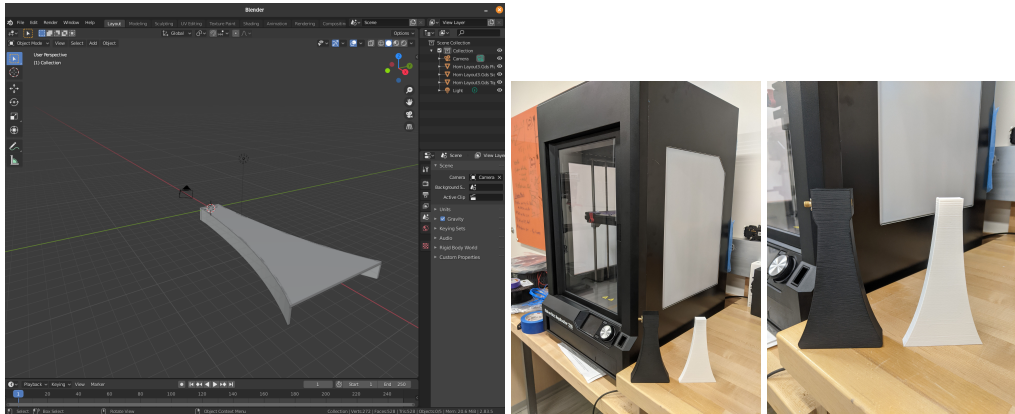


Figure 1.4: (Left) Blender/STL files extracted from MEEP code. (Middle) MakerBot 3D printer, with PLA horn model (white), and proto-pasta with SMA connector (black). (Right) Close-up of horns.

In Summer 2021, we received a second ONR fellowship to continue the research. We determined how to integrate CAD design with MEEP in 2D, and later 3D. As a result, we can now simulate the radiation patterns and S-parameters of the exact object we hope to print. We acquired NinjaTek proto-pasta 3D printer filament, advertised as conductive. We printed a horn with in-built SMA connector for RF cables (Fig. 1.4). The proto-pasta result had a measured resistance of $\approx 10 \text{ k}\Omega$, too large for an RF antenna. Multi3D LLC, the manufacturer of the Electrifi filament, has now provided resistivity results that compare proto-pasta with Electrifi (Fig. 1.5). The Electrifi filament will improve resistivity by two orders of magnitude. We seek to print new RF antennas, and to measure the radiation pattern and S-parameters.

In Summer 2022, we received a third ONR fellowship focusing on GPS modernization². Alongside this work, we continued to refine the open-source CEM results. We learned to simulate the full 3D horns stored in CAD files using parallel processing, achieving an order of magnitude reduction in computation time. The results are shown in Fig. 1.6. In Fig. 1.6 (a), the main lobes are designed to point to 0 degrees (x-direction) for the E-plane (x-y plane), and 90 degrees for the H-plane (x-z plane). The E-plane contains the linearly polarized radiation vector. In Fig. 1.6 (b), the voltage standing wave ratio (VSWR) is shown.

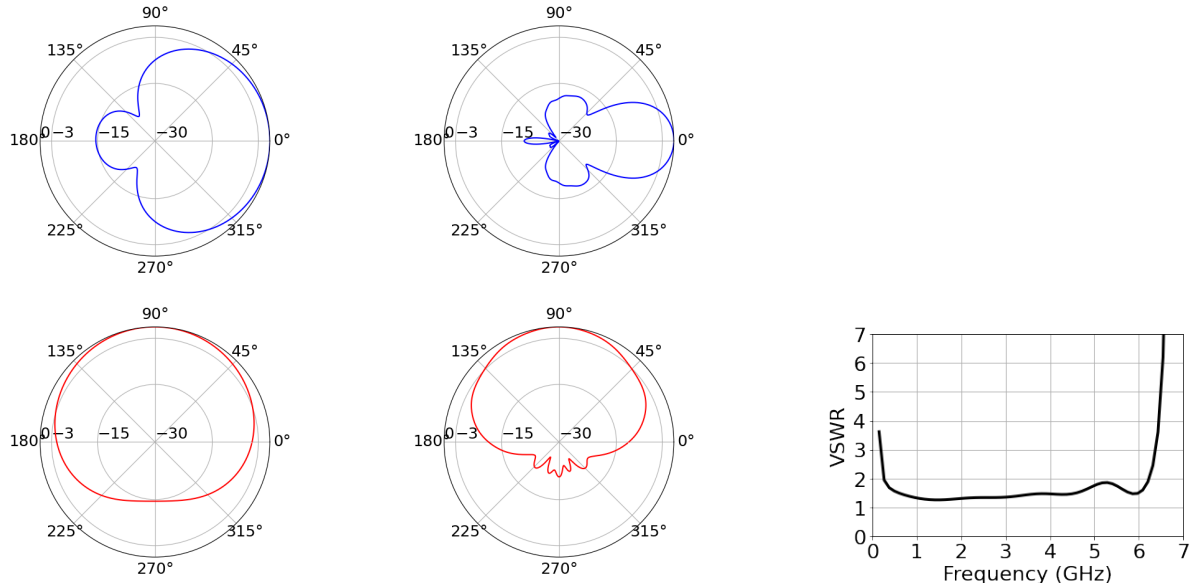
²ONR regulations state that a gap year is required. For our group, Senior Fellowship eligibility begins in Summer 2024.

Horizontal Traces	Dimension (X × Y × Z cm ³)	Resistance (Ω)	Resistivity (Ω cm)
Electrifi	0.2 × 10 × 0.2	3.0	0.012
Black Magic 3D	0.2 × 10 × 0.2	142.5	0.57
Proto-Pasta	0.2 × 10 × 0.2	1506	6.02

Vertical Towers	Dimension (X × Y × Z cm ³)	Resistance (Ω)	Resistivity (Ω cm)
Electrifi	0.5 × 0.5 × 10	3.4	0.085
Black Magic 3D	0.5 × 0.5 × 10	103.6	2.59
Proto-Pasta	0.5 × 0.5 × 10	410	10.25

Figure 1.5: Resistivity results published by Multi3D LLC that compare the proto-pasta product with the new Electrifi conductive filament (<https://www.multi3dllc.com/faqs/>).

The VSWR is a common figure of merit for RF antennas, related to the S-parameters. The VSWR approaches 1 for an efficiently radiating antenna, and infinity for no efficiency. The radiation patterns match expectations for horn antennas (see Fig. 19 of [10]). The VSWR results demonstrate efficient radiation in the bandwidth [0.5 - 6] GHz. We presented our progress at the annual MeepCon 2022 at the Massachusetts Institute of Technology (MIT) [11]. We learned new techniques for integrating MEEP and machine learning tools [29], and how eager MEEP developers are to collaborate in the RF regime.



(a) Radiation pattern results using GDSII/CAD for (top left) E-plane at 0.5 GHz, (top right) E-plane at 5.0 GHz, (bottom left) H-plane at 0.5 GHz, (bottom right) H-plane at 5.0 GHz. See text for details.

(b) The VSWR figure of merit versus frequency in GHz for the RF horn.

Figure 1.6: Results for RF horn design, using open-source CEM software, and a 3D CAD design process open to 3D printing.

1.1.1 RF Laboratory Capability and Prior ONR Funding

We are required to take a research gap year in Summer 2023, according to ONR regulations. However, we have now begun an Educational Partnership Agreement (EPA) between NSWC Corona and Whittier

Equipment	Bandwidth	Cost
Rohde and Schwartz ZVL6 Network Analyzer	9 kHz to 6 GHz	\$20k
Rohde and Schwartz NRP-91 Power Sensors (2)	9 kHz to 6 GHz	\$8k
Aeroflex 3416 Digital RF Signal Generator	250kHz to 6 GHz	\$12k
Calibration antenna kits (2)	Varies by antenna	\$2k
Calibration test kits for Network Analyzer (2)	6 kHz to 9 GHz	\$6k

Table 1.1: A listing of the equipment provided to our labs by the Office of Naval Research.

Student/Professor	Grant Opportunity	Amount	Dates
Jordan C. Hanson	ONR Summer Faculty Fellow	\$16.5k	Summer 2022
Dane Goodman	Summer researcher	Course credit	Summer 2022
Andrew Householder	Summer researcher	Course credit	Summer 2022
Raymond Hartig	Ondrasik-Groce Fellowship	\$5k	Summer 2022
Jordan C. Hanson	ONR Summer Faculty Fellow	\$16.5k	Summer 2021
Adam Wildanger	Fletcher Jones Fellowship	\$5k	Summer 2021
Jordan C. Hanson	ONR Summer Faculty Fellow	\$16.5k	Summer 2020
Raymond Hartig	Fletcher Jones Fellowship	\$5k	Summer 2020
John Paul Gómez-Reed	Ondrasik-Groce Fellowship	\$7.5k	Summer-Fall 2019
John Paul Gómez-Reed	Keck Fellowship	\$5k	Summer 2018
Cassady Smith	Keck Fellowship	\$5k	Summer 2018

Table 1.2: A listing of the grant opportunities awarded to our group for RF design, software development, and machine-learning. All students are at the undergraduate level.

College. NSWC Corona now has the ability to transfer laboratory equipment to Whittier College. NSWC Corona has provided RF bench testing equipment that is perfectly suited to the proposed work. A list of instruments transferred from NSWC Corona between 2020 and 2023 is shown in Tab. 1.1. Our network analyzer and power sensors can perform S-parameter measurements over [9 kHz - 6 GHz] for our antennas under test (AUT). Our signal generator can create calibration signals for our calibration antennas and AUT over [250 kHz - 6 GHz]. Our calibration antennas serve as benchmark devices for comparison to our 3D printed AUT. Due to the precision and wide bandwidth of these devices, regular calibration is required. Our calibration kits serve this purpose. Our laboratory is therefore well-equipped to complete the proposed work, and this minimizes budgetary impact.

This research has been completed with significant contributions from diverse undergraduate students. We provide a summary of funding for personnel that have contributed to the early stages of this work in Tab. 1.2. These researchers have diverse majors and interests, including our 3-2 Engineering Program (Wildanger), Physics and Math double major (Hartig), and Math/Integrated Computer Science (Gómez-Reed and Householder), and Physics and Astronomy (Goodman and Smith). After Whittier College, these students have begun science and engineering roles that include the Laser Interferometer Gravitational-Wave Observatory (LIGO), the University of Southern California (USC), and The Aerospace Corporation. Whittier College has a good track record of providing access to higher education, and careers in science and technology, to diverse students from Los Angeles County and beyond.

1.2 The Connection to Ultra-High Energy Neutrino Observations

The flux of neutrinos with energies between [0.01-1] PeV (10^{15} eV) has been detected by IceCube [30]. The UHE- ν flux, with energies above 1 PeV, could explain the unknown origin of UHE cosmic rays (UHECR) [31]. This flux also represents an opportunity to study electroweak interactions at record-breaking energies [32]. Previous analyses have shown that the discovery of UHE- ν will require an expansion in detector volume, because the UHE- ν flux is expected to decrease with energy [33–37]. Whereas the current version of IceCube detector observes neutrinos via optical signals that travel < 100 m,

the Askaryan effect translates a UHE- ν interaction into an RF pulse that travels more than 1 km in dielectric media such as Antarctic and Greenlandic ice [38–42].

Utilizing the Askaryan effect therefore allows for detectors with vastly larger effective volumes than optical observations. Arrays of $\mathcal{O}(100)$ *in situ* detectors encompassing effective areas of $\approx 10^4 \text{ m}^2$ steradian per station, spaced by $\mathcal{O}(1)$ RF attenuation length could discover a UHE- ν flux beyond the limits of the EHE analysis. Polar ice formations in Antarctica and Greenland have the longest RF attenuation lengths. A group of prototype Askaryan-class detectors has been deployed in polar regions that seek to probe unexplored UHE- ν flux parameter-space [36, 37, 43, 44].

Askaryan radiation was first observed in laboratory settings [45–47]. Working with an undergraduate researcher, we recently published a theoretical model of the electromagnetic field of Askaryan radiation [48]. Askaryan models are incorporated into simulations like AraSim in order to calculate expected signals and aid in detector design [49–51]. Software developed for IceCube Gen2 (radio) utilizes machine learning and the Askaryan pulse shape to reconstruct UHE- ν properties in future data [14, 52, 53]. Askaryan electromagnetic fields are combined with RF channel responses to form “signal templates” used to search large data sets for signal candidates [36, 54]. Data sets are large for Askaryan-class detectors due to the inevitable RF thermal background data. Askaryan signal SNRs at RF channels are expected to be small ($\text{SNR} \approx 3$) [40, 55, 56]. Template-waveform matching between models and data is a powerful technique for isolating the small signals [36, 54, 57, 58].

Given the expected signal SNR, phased arrays have been incorporated into Askaryan-class prototype detectors [1, 2]. As described at the beginning of Sec. 1, phased arrays boost the signal SNR. Examples of this strategy are ARA5 [13], and the first deployments of Radio Neutrino Observatory, Greenland (RNO-G) [59]. The arrays in each consist of identical, vertically polarized dipoles. These decisions were made for mechanical reasons, because the array must fit in a 100 m deep, vertically-drilled borehole in the ice. The radiation pattern exhibits azimuthal symmetry, and there is minimal sensitivity to the horizontal Askaryan field component. Further, the designs assume a uniform index of refraction for the ice surrounding the array. As part of our proposed work, we seek to use machine learning to discover horizontally polarized array designs that fit into the borehole and account for the index of refraction, n .

We included a short study of phased array behavior in the South Pole ice environment in our recent publications [3, 12]. Most commercial CEM packages assume a uniform n in the surrounding medium. By contrast, MEEP gives the user 3D control of the index of refraction, $n(x, y, z)$. The RF index of refraction varies with the depth (z) near the snow surface. The $n(z)$ function is well-measured in a variety of locations in Antarctica [60], and Greenland [61]. ARA (South Pole), RNO-G (Greenland), and IceCube Gen2 (radio) (South Pole) can all benefit from designs that account for $n(z)$ and have sensitivity to the horizontal component of the Askaryan field. There is an ongoing effort to reconstruct the polarization of incoming test signals through South Pole ice, in order to more tightly constrain future UHE- ν observations [14].

The common simulation package used for ARA, RNO-G, and IceCube Gen2 is now NuRadioMC, built from prior experience with ARA and ARIANNA [37, 42, 51, 62, 63]. NuRadioMC addresses analytically the ray-tracing solution for UHE- ν signals as they propagate through polar ice. We derived the analytic ray-tracing solutions presented in [51] and [60], which were adopted into NuRadioMC. A goal of our proposed research will be to incorporate realistic, 3D field propagation into NuRadioMC using FDTD computations with MEEP, with our analytic Askaryan model as the MEEP source [48, 64]. This integration should boost the accuracy of the computations made with NuRadioMC, which will be matched with future ARA, RNO-G, and IceCube Gen2 data to isolate UHE- ν signals.

1.3 The Connection to Remote Sensing of Ice Sheets

A gap exists in Askaryan-based UHE- ν science that connects to the remote sensing of ice sheets. A knowledge of the RF attenuation length, λ , versus frequency, depth, and location is paramount to understanding UHE- ν detector sensitivity. Although we have made detailed measurements of λ versus



Figure 1.7: Our 3D-printed quad-rotor drone, designed and assembled by Whittier College undergraduates using our RF design lab and machine shop. The unit is equipped with hand-held RC control, and GPS with programmable waypoints.

frequency [40,41,65], we do not scan detector volumes to measure this parameter versus geographic location: $\lambda(x, y)$. Further, $\lambda(z)$ is merely inferred from depth-averaged attenuation measurements and ice core temperature data (see Fig. 24 from [42]). IceCube Gen2 (radio) will require $\lambda(x, y, z)$ to be measured precisely. CReSIS radio sounding data, available on the Open Polar Server (OPS:

<https://ops.cresis.ku.edu/>), have been used to constrain $\lambda(x, y)$ across Greenland [66]. Far less CReSIS data is available near the South Pole, due to the complex logistics of organizing flights in that region. Such logistical challenges are one of several factors motivating a new effort to incorporate radio sounding instrumentation into unmanned aerial systems (UAS).

UAS systems offer a way to enrich radio sounding data for geophysics and particle astrophysics. In the past, radio sounding data has been generated from human-piloted fixed-wing aircraft with straight flight lines that carry on-board radar. Flight lines can be hundreds of kilometers long, scanning wide areas with synthetic aperture radar (SAR) techniques. There are, however, three key disadvantages. First, there may not be a flight near the desired location (e.g. South Pole). Second, flights only give a single snapshot in time, and aircraft may not return to the site for years. Third, the radar bandwidth does not always overlap with the science bandwidth of (for example) IceCube Gen2. Dedicated UAS could constrain $\lambda(x, y)$ in both the temporal and spatial regimes. UAS are able to hover and fly at lower altitudes, so they can collect a wider variety of data than fixed-wing craft. For example, the CReSIS ultra-wide band (UWB) Snow Mini radar system was integrated onto the AeroVironment Vapor 55 UAS. The low altitude flight capability increases the SNR in difficult areas by pushing clutter angles outside the field of view. The SNR is also boosted by hovering due to increased integration time over the site [5]. The average cost of the Vapor 55, however, is about \$90k USD.

In our RF design lab at Whittier College, our group has already constructed a 3D printed drone using PLA, carbon-fiber tubing, commercial motors, and commercial transceivers. The unit has ≈ 1 kg payload and a 20-min flight time powered by LiPo batteries. The total cost is ≈ 1 k USD (see Fig. 1.7). Before the onset of the COVID-19 pandemic paused in-person work, we had plans to equip it with solar charging and cold-temperature components. Thus, there is a potential for collaboration between CReSIS and IceCube Gen2 (radio) to solve a common problem: the solar rechargeable $\lambda(x, y)$ measurement system with vertical take-off and landing (VTOL). Our drone design with VTOL capability can be 3D printed and assembled from commercial parts for ≈ 1 k. We hope to collaborate with the CReSIS group on retro-fitting for cold temperatures and solar charging. When outfitted with a 3D-printed phased array radar, we will have a formidable system capable of filling gaps in our knowledge of polar ice sheets.

The incorporation of phased array radio sounding systems on UAS faces an optimization problem: the right balance between craft weight, thrust, payload, and flight time must be achieved. To collect quality radio sounding data, the payload must be flown horizontally for 1 – 10 km, implying ≈ 1 hr battery life at reasonable speeds. Longer flight times require larger batteries. Increased battery size increases weight,

which tends to decrease flight time. Phased array payloads with a large number of elements could benefit data collection, but this adds weight and decreases flight time. The optimization is made far easier if the phased array system is integrated into the hull of the UAS. We propose to study how the RF phased array can be printed into the hull of the UAS, using machine learning to optimize beam-forming for radio sounding. The Electrifi filament has a similar density to aluminum, meaning it can serve as *both* a structural component and a phased array material. Manufacturing structural components as phased array elements reduces costs, weight, and payload. Through this research, we seek to advance the ongoing CReSIS effort to miniaturize radar units for UAS integration.

As part of this engineering effort, we also propose to simulate expected results using MEEP. Performing a CEM simulation that incorporates our current knowledge of ice properties with the UAS radar response would enrich the research in two ways. First, such simulations enhance the design process, revealing design requirements, shortcomings, and ways to overcome them. MEEP simulations require the user to specify the complex matrix for the dielectric constant of the medium, $\epsilon(x, y, z)$. The ϵ matrix determines how RF waves reflect, refract, and propagate back to the receiver. Optimizing UAS phased array design for maximal $\epsilon(x, y, z)$ precision will result in optimal precision for $\lambda(x, y, z)$. For dielectric materials, ϵ and λ are related analytically [40]. Second, building such MEEP simulations will provide a cross-check between the observed $\epsilon(x, y, z)$ from field data, and the simulated $\epsilon(x, y, z)$.

FDTD simulations are notorious for consuming computational resources like volatile memory, while providing the necessary resolution for $\epsilon(x, y, z)$, and electromagnetic fields versus time, frequency, and space. We have acquired a System76 Helio desktop system with AMD Ryzen threadripper 3990x 64-core, 128 thread processor. The system has 0.5 GB of volatile memory per thread. We have already shown that running MEEP in parallel on our system reduces run times by an order of magnitude [11]. The reduction is due primarily to increased set up speed for $\epsilon(x, y, z)$. Thus, we are already in a position to perform such CEM simulations quickly and efficiently. Learning how to introduce parallelism into computational problems will also be of educational benefit to our STEM undergraduates at Whittier College. In fact, the introduction of new concepts related to our research within STEM courses at Whittier College is a main goal of our proposal.

1.4 Integration of Research and Education at Whittier College

The integration of our proposed research into our STEM curriculum will benefit our diverse undergraduates in two ways. The first benefit is the boosted engagement derived from integrating real applications of physics and computer science into our courses. The second benefit is the creation of undergraduate research opportunities, providing a venue for students to grow and apply their skills. Course integrations will take place within our Department of Physics and Astronomy, and others will take place in the Department of Mathematics and Computer Science. We will work with our colleagues to integrate this research into courses like Computer Logic and Digital Circuit Design, Digital Signal Processing, Machine Learning, and Introduction to Data Science with Python. I personally teach two of these courses, and I note below when collaboration with another instructor is required. We already have faculty in Math and Computer Science who specialize in machine learning. For example, Prof. Fred Park specializes in the application of machine learning and parallel computing to computer vision and image analysis [67,68]. Finally, we already have a track record of success with undergraduate research fellowships (see Tab. 1.2). Our students have made wonderful achievements in CEM, firmware design, and theoretical physics with our local Ondrasik-Groce and Fletcher Jones Fellowships. Our goal is to expand this practice through NSF-sponsored opportunities in additive manufacturing, CEM, and machine learning.

1.4.1 Course Integrations - Electromagnetism and Computational Physics

Course integrations that will take place within the Department of Physics and Astronomy are Algebra-Based Physics II (Electricity, Magnetism, and Modern Physics), Calculus-based Physics II

(Electromagnetism), Electromagnetic Theory, Optics, and Computational Physics³. The first two courses represent the standard introductory level content on electromagnetism. Simple web-based learning modules will be developed to illustrate the concepts of electromagnetic waves and optics via MEEP in Jupyter notebooks (<https://jupyter.org/>). Jupyter is a cross-platform open-source project that supports interactive data science and scientific computing. We have experience creating and sharing MEEP notebooks in Jupyter to accomplish research [3], and in teaching Computer Logic and Digital Circuit Design using the PYNQ-Z1 SoC (<http://www.pynq.io/>). Such notebooks are easily integrated into Moodle, our web-based content management system (CMS), because they are web-based. The primary learning enhancement is to illustrate dynamic electromagnetic fields that can be shown alongside textbook examples. The students can therefore compare their theoretical understanding with a visual representation. Their final projects in these courses are self-designed DIY physics experiments in DC circuits, optics, and magnetism. We look forward to students accepting the challenge of matching simulation output to their real-world results.

We submit reflective analyses of our teaching, research, service, and advising every two years as part of our standard process for tenure and promotion. My teaching reflections have revealed the learning value of the synergies between traditional lecture content, simulations, and lab experiments. Students in Algebra-Based and Calculus-Based Physics are fully prepared to apply ideas of physics in their own projects when the ideas solidify in their minds. Solidification occurs when they demonstrate them as theoretical predictions, simulate them, and test them in the lab. After solidification, learning anxiety fades, and students feel comfortable applying concepts. A good example is DC circuit analysis. We first solve systems of equations that predict currents through multiple devices connected to a battery. In a popular PhET simulation, PhET DC Circuit Construction Kit, current and charge are animated, and students can make virtual (simulated) measurements. The students replicate the virtual circuit in the lab, and show that the volts and amps in real life match the simulation. There are, however, few HTML5 PhET simulations that illustrate dynamic electromagnetic fields. We can use Jupyter modules with MEEP to fill this gap. For a variety of references on the use of technology in STEM education, see [17].

We have three opportunities to integrate our research within advanced physics courses: Optics, Electromagnetic Theory, and Computational Physics. Our Optics course introduces students to three areas. The first is ray optics, with discussions of lenses and optical instruments. The second is wave optics, with discussions of superposition, interference, and diffraction. The third is modern optics, with discussions of photons, spectra, lasers, interferometry, fiber optics, and nonlinear optics. One useful Jupyter module incorporating MEEP into ray optics would be a lens example demonstrating focal length. As the course progresses to wave optics, the lens example could be enhanced more complex, photonics examples [69]. The modern optics curricula presents rich opportunities to use Jupyter and MEEP to illustrate course concepts. Some examples include flux and spectral monitoring for diffraction gratings [70], and waveguides for fiber optics [71]. Most Optics students have taken Computer Science 1 (Python3) and one semester of Modern Physics, so combining Python and electromagnetism should be achievable. I do not personally teach this course, but I can collaborate with the instructor. Our small department has a good track record of collaboration.

The course integration in Electromagnetic Theory carries great potential. This one-semester course usually covers chapters 1-7 of *Introduction to Electrodynamics* by D. Griffiths (Cambridge University Press, 2017), with some examples of electromagnetic waves. Students are exposed first to electromagnetic waves in the prerequisite Modern Physics, and the advanced course gives a minor elaboration on waves in vacuum. Using Jupyter modules with MEEP, we can easily introduce waves interacting with non-uniform dielectric media. The difference between ray-tracing and true three-dimensional propagation in polar ice with $n(x, y, z)$ is an excellent example of how the UHE- ν research, CEM, and teaching intersect (see Sec. 1.2). Many examples in the MEEP documentation serve as starting points for these modules. One example, “the S-parameters of a directional coupler,” is a system of waveguides that provided basic code for computing the S-parameters of our RF antenna designs [11]. Finally, we can introduce a Jupyter module

³I personally teach Algebra-Based Physics II, Calculus-Based Physics II, and Electromagnetic Theory. Optics and Computational Physics are normally taught by my colleagues within Physics and Astronomy. Computational Physics will soon be handed to myself and others as the usual instructor retires.

encompassing specular and diffuse reflection from rough surfaces. This module would form a connection between CReSIS radio sounding research, CEM, and teaching (see Sec. 1.3). In all physics and engineering courses, the phase arrays we produce can be showcased as a practical application of electromagnetic theory.

1.4.2 Course Integrations - Computer Logic and Digital Circuit Design, and Digital Signal Processing

Since I arrived at Whittier College in 2017, I created two computer science courses: Computer Logic and Digital Circuit Design, and Digital Signal Processing. The former covers number systems, Boolean algebra and complex logic functions, adders, encoders, comparators, shift-registers and memory, counters, finite state machines, timing diagrams, firmware programming with Python, and lab techniques for digital circuits, and ADC/DAC. The laboratory component of this course is performed on the PYNQ-Z1 SoC (<http://www.pynq.io/>), allowing students to write firmware in Python. Examples of laboratory activities in this course include creating digital logic functions with LED outputs and ADC/DAC examples with Digilent PMODs. There are a plethora of examples with the PYNQ community that implement neural networks and image/video processing using FPGA acceleration. Many of the students who take this course are actively seeking research opportunities, and one interesting possibility for a course integration is to incorporate FPGA acceleration into machine learning and CEM calculations. It is possible to run Jupyter, MEEP, and FPGA acceleration code simultaneously on the PYNQ-Z1 boards in our teaching labs. Boosting these aspects of the course will therefore enhance education and research through student-driven projects involving FPGA acceleration.

Digital Signal Processing (DSP) is another course I have created. Among the topics covered are statistics and probability, complex numbers, noise in digital systems, ADC/DAC, sampling and digitization, Fourier series, Fourier and discrete Fourier transforms (DFTs), Laplace and z-transforms, linear time-invariant (LTI) systems and filtering, audio and image processing, applications to digital circuits, and applications of neural networks. Though this course was originally created independently of Computer Logic and Digital Circuit Design, it has evolved to become a continuation of it. These two courses can take students all the way from basic binary to understanding digitized, sampled signals with complex analysis. An interesting course integration between DSP and our CEM research is the application of DFTs to MEEP flux monitors and near-to-far-field monitors. These are objects that compute and project the radiation flux passing through a surface as a function of frequency using DFTs. Students will learn that the radiation is nothing more than a digitized sampled signal within a CEM context, and that the DFT is a tool for understanding spectra. We can adapt Jupyter modules we have already written to this task.

1.4.3 Course Integrations - Introduction to Data Science with Python, and Machine Learning

There are two additional courses within the mathematics and computer science that represent integration opportunities: Introduction to Data Science with Python, and Machine Learning. The former is an introductory course that assumes the student has basic programming skills. Students learn import, explore, analyze, and visualize data using tools like Jupyter notebooks, NumPy, and Matplotlib. More advanced tools like Pandas, SciPy, and scikit-learn are introduced. There are several straightforward enhancements that can be provided with Jupyter notebooks that demonstrate CEM. Quantities like radiation patterns and S-parameters are fertile grounds for learning to visualize data with Matplotlib. We have published such visualizations, and we can share this experience [3]. Scikit-learn is already included in the syllabus, so RF antenna optimization with basic machine learning tools is also straightforward. This course is taught by Prof. Glenn Piner, who is our colleague in the Department of Physics and Astronomy. By working together to incorporate these ideas as appropriate into this introductory course, our students will gain early preparation to perform the cutting edge research with MEEP and additive manufacturing. Once the RF antennas are manufactured, we can conduct in-class demonstrations to inspire the students with a real world application.

Discipline	GPA (Students of Color)	GPA (White)	Shift
Physics	2.62	3.15	-0.53
Mathematics	2.54	2.75	-0.21
Computer Science	2.77	3.31	-0.54
Chemistry	3.02	3.20	-0.18
Biology	3.03	3.18	-0.15
Environmental Science	3.17	3.25	-0.08

Table 1.3: GPA data for Whittier College students from Fall 2016 to Spring 2021, disaggregated by racial background and discipline. See text for details.

The final course opportunity for course integration is Machine Learning. Typically taught by Prof. Fred Park, this course assumes a more advanced knowledge of Python and Calculus II. Topics include unsupervised and supervised learning, data clustering, principle component analysis, logistic regression, support vector machines, neural networks, and deep learning. One topic that might prove a useful addition to the syllabus is *genetic programming*. Genetic programming has been used to optimize RF antennas [72, 73]. We will work together to incorporate genetic programming as appropriate into the syllabus. As with Data Science, demonstrations of the optimized RF antenna would be ideal. We seek to demonstrate a practical application of machine learning in the fields of physics, geophysics, and climate science. This course is in high demand because students understand the large number of opportunities that await them in the defense and software development sectors in Southern California. One such opportunity will be our newly created EPA with NSWC Corona. Our students will be doubly prepared with the engineering experience from the RF application, and the machine learning training.

1.5 Translation of STEM Research for our Community

Our proposed project will provide valuable opportunities to diverse students from our community, which is heavily influenced by our bilingual families. Families that speak Spanish at home and English at school are very common at Whittier College (an HSI). For Fall 2022 admitted students, 36% are Hispanic/Latino, and another 8% are International students. Over the past five years, students of color and first-generation students have comprised 69% and 34% of the student body, respectively. We have observed that students of color receive lower grades than their peers in our introductory STEM courses (see Tab. 1.3). We have learned from workshops that emphasizing the dignity and self-efficacy of the student works against disparity [15, 16]. In keeping with the project theme of *translation* of progress in one area to serve another, and in order to emphasize the dignity of our students no matter their background or the adversity they encounter, we seek to produce a bilingual mobile application introducing STEM concepts within a welcoming digital environment.

Implementation of the Duolingo method for language and mathematics on a mass scale has provided promising results [17]. Results presented within the educational data mining (EDM) literature provides additional examples of apps and techniques that boost engagement and success in introductory STEM courses [18–21]. Some members of our community have shared that translating mathematics and physics exercises into Spanish aids in solving them. Our app will boost their skills and build confidence by offering them engaging, game-like physics training in the language of their choice. Even if the base language of STEM content in our courses does not represent a barrier for our students, the design of our app, based on the Duolingo Method, should boost the skill of all our students.

The Duolingo method has five main components [17]. The first component is Learning by Doing, or utilizing the innate learning toolkit every student has. Learning by doing also involves affordance-based design, embodied cognition, and explicit instruction. The second component is to Learn in a Personalized Way. This involves utilizing machine learning to ensure content is just difficult enough for the individual student to grow, but not so difficult that the student becomes disengaged. The distinction hinges on “desirable” difficulty, versus “undesirable” difficulty. The third component is to Focus on What Matters. This component is about ensuring course content is matched to verified learning standards like Common Core. The fourth component is to Stay Motivated. Using game-like design with points, rewards,

leaderboards, and collaboration has been shown to motivate students in a positive way. The fifth is to Feel the Delight. This component is many things: quality storytelling, including diverse characters within the app, and providing moral encouragement. The key is to create a positive environment conducive to learning.

Two additional themes are relevant for mathematics learning in the Duolingo method: using multiple mathematical representations for the same concept (see Sec. 1.4.1), and the manipulation of tools. Both themes follow the concrete-real-abstract (CRA) learning progression. A CRA progression is used to guide students towards understanding abstract mathematical concepts by first introducing them with concrete tools or representations, and gradually increasing the level of abstraction. According to the authors, “Equations, pictures, and narratives can all be used to describe mathematical concepts. Moreover, using multiple representations supports learners’ analogical thinking abilities ... Because these representations also are at varying levels of abstraction, we construct lessons so learners experience representations which are closer to real objects before they interact with more abstract representations” [17].

Once implemented, we have two goals for the app. First, we seek to test the *hypotheses* that the Duolingo method, and the two additional math themes, will boost the GPA results in Tab. 1.3 and reduce disparities. Second, we seek to affirm our students’ dignity and cultural identity by making the app bilingual. We hope these twin goals will serve to build confidence in our students by welcoming them into STEM learning at the college level.

Educational Application for Student Learning of STEM (EASTLOS). A prototype application, code-named EASTLOS for “East Los Angeles” (our geo-cultural area) is being built by Whittier College undergraduates. The software and digital design of the app represents an opportunity for Whittier College students to enhance the learning experience for their peers while gaining valuable work experience. In our budget and project planning we include paid student positions for code and digital design, and allocate time and space to finish the application. By recruiting and using home-grown talent, we hope to inspire a passionate set of diverse software designers to help implement and disseminate the app. We include three general phases in our project planning (Sec. 1.7). (1) We will design and implement the app for an introductory physics course. (2) We will use the app to gather data and make improvements. (3) We will present results to a broader audience, and help to implement the app in other courses and in the wider community.

1.6 Bilingual Public Lectures and Recruitment Events

Example

1.7 Timeline and Project Planning

An example figure.

[Open-Source CEM and Additive Manufacturing, Year 1]
 [Whittier College]
 [Profs. J. Hanson, F. Park, S. Zorba, S. Lagan, G. Piner]
 [Nayeli Camacho, Shaun Dunnick]

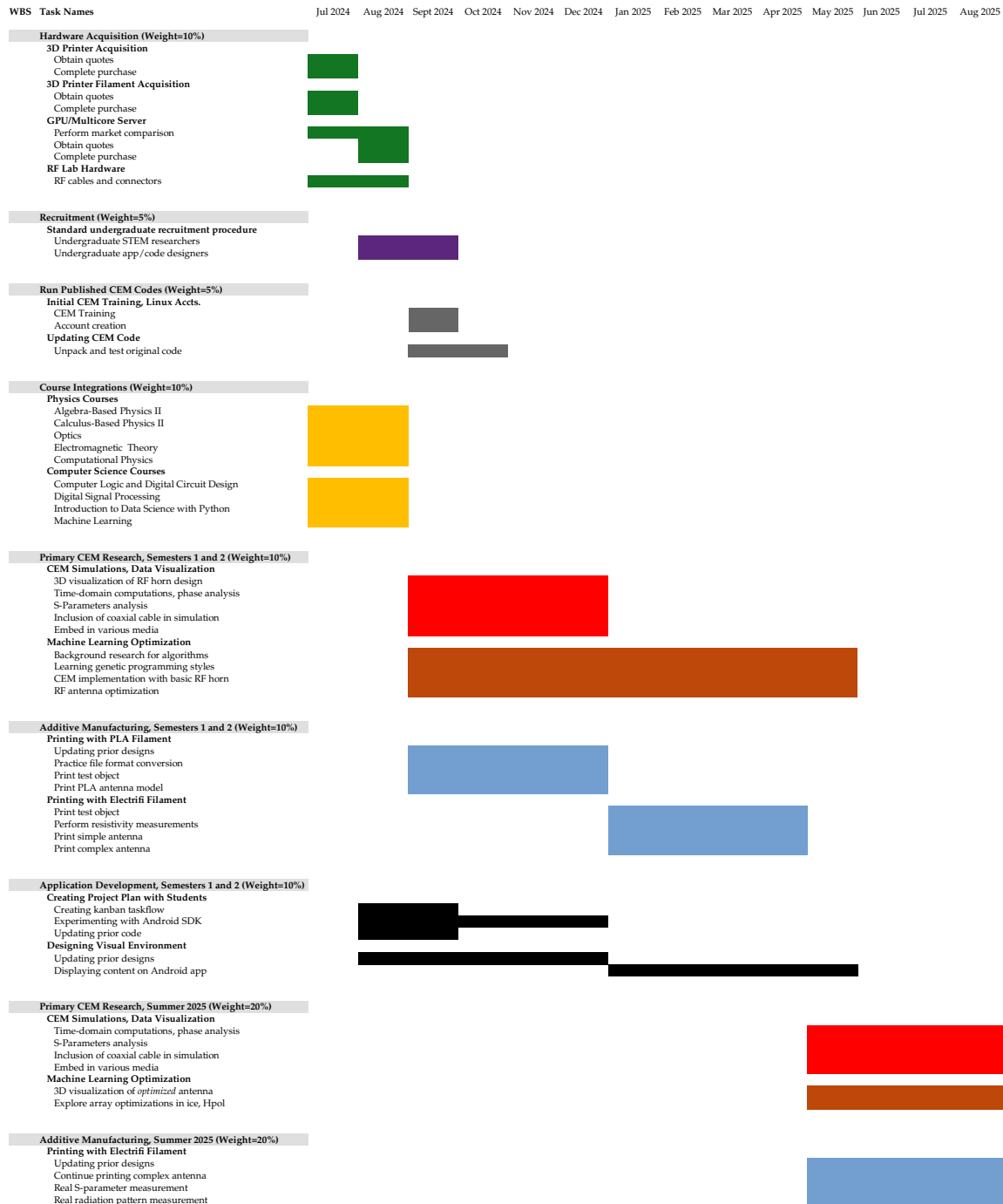


Figure 1.8: A Gantt chart outlining project planning, in visual form, for Year 1 of the project.

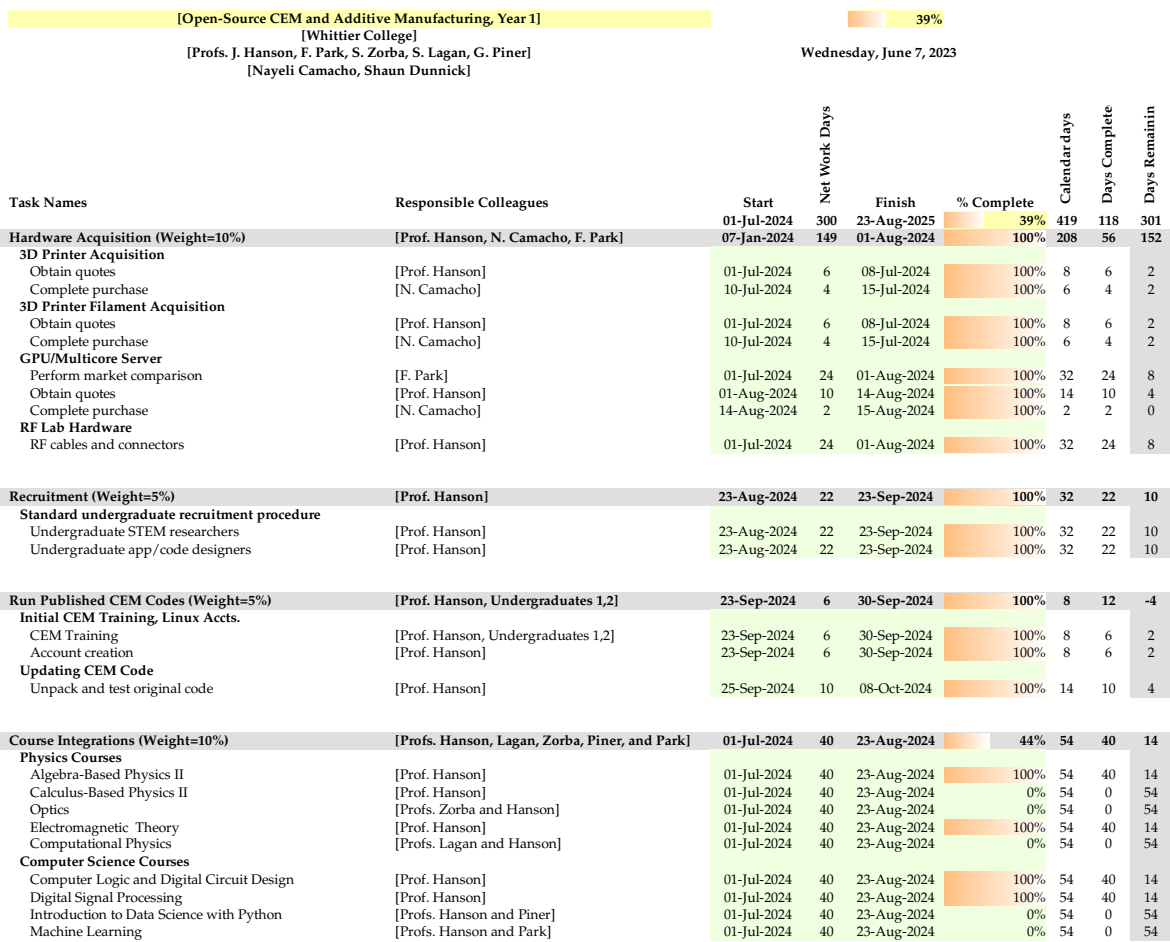


Figure 1.9: A Gantt chart outlining project planning, in numerical form, for Year 1 of the project (part 1).



Figure 1.10: A Gantt chart outlining project planning, in numerical form, for Year 1 of the project (part 2).

Bibliography

- [1] A. Vieregg, K. Bechtol, and A. Romero-Wolf, "A technique for detection of pev neutrinos using a phased radio array," *Journal of Cosmology and Astroparticle Physics*, vol. 2016, p. 005, feb 2016.
- [2] J. Avva, K. Bechtol, T. Chesebro, L. Cremonesi, C. Deaconu, A. Gupta, A. Ludwig, W. Messino, C. Miki, R. Nichol, E. Oberla, M. Ransom, A. Romero-Wolf, D. Saltzberg, C. Schlupf, N. Shipp, G. Varner, A. Vieregg, and S. Wissel, "Development toward a ground-based interferometric phased array for radio detection of high energy neutrinos," *Nuclear Instruments and Methods in Physics Research Section A: Accelerators, Spectrometers, Detectors and Associated Equipment*, vol. 869, pp. 46–55, 2017.
- [3] J. C. Hanson, "Broadband rf phased array design with meep: Comparisons to array theory in two and three dimensions," *Electronics*, vol. 10, no. 4, 2021.
- [4] J. Aguilar, P. Allison, J. Beatty, H. Bernhoff, D. Besson, N. Bingefors, O. Botner, S. Buitink, K. Carter, B. Clark, A. Connolly, P. Dasgupta, S. de Kockere, K. de Vries, C. Deaconu, M. DuVernois, N. Feigl, D. García-Fernández, C. Glaser, A. Hallgren, S. Hallmann, J. Hanson, B. Hendricks, B. Hokanson-Fasig, C. Hornhuber, K. Hughes, A. Karle, J. Kelley, S. Klein, R. Krebs, R. Lahmann, M. Magnuson, T. Meures, Z. Meyers, A. Nelles, A. Novikov, E. Oberla, B. Oeyen, H. Pandya, I. Plaisier, L. Pyras, D. Ryckbosch, O. Scholten, D. Seckel, D. Smith, D. Southall, J. Torres, S. Toscano, D. V. D. Broeck, N. van Eijndhoven, A. Vieregg, C. Welling, S. Wissel, R. Young, and A. Zink, "Design and sensitivity of the radio neutrino observatory in greenland (RNO-g)," *Journal of Instrumentation*, vol. 16, p. P03025, mar 2021.
- [5] E. Arnold, C. Leuschen, F. Rodriguez-Morales, J. Li, J. Paden, R. Hale, and S. Keshmiri, "Cresis airborne radars and platforms for ice and snow sounding," *Annals of Glaciology*, vol. 61, no. 81, p. 58–67, 2020.
- [6] L. Li, J.-B. Yan, C. O'Neill, C. D. Simpson, and S. P. Gogineni, "Coplanar side-fed tightly coupled ultra-wideband array for polar ice sounding," *IEEE Transactions on Antennas and Propagation*, vol. 70, no. 6, pp. 4331–4341, 2022.
- [7] S. Hussain, S.-W. Qu, A. Sharif, H. Abubakar, X.-H. Wang, M. Imran, and Q. Abbasi, "Current sheet antenna array and 5g: Challenges, recent trends, developments, and future directions," *Sensors*, vol. 22, no. 9, 2022.
- [8] A. Fedeli, C. Montecucco, and G. L. Gragnani, "Open-Source Software for Electromagnetic Scattering Simulation: The Case of Antenna Design," *Electronics*, vol. 8, no. 12, p. 1506, 2019.
- [9] O. Yurduseven, S. Ye, T. Fromenteze, B. Wiley, and D. Smith, "3d conductive polymer printed metasurface antenna for fresnel focusing," *Designs*, vol. 3, no. 46, 2019.
- [10] F. Pizarro, R. Salazar, E. Rajo-Iglesias, M. Rodríguez, S. Fingerhuth, and G. Hermosilla, "Parametric study of 3d additive printing parameters using conductive filaments on microwave topologies," *IEEE Access*, vol. 7, pp. 106814–106823, 2019.
- [11] J. Hanson, "Broadband rf phased array design with meep." MeepCon 2022, 2022.
- [12] A. F. Oskooi, D. Roundy, M. Ibanescu, P. Bermel, J. Joannopoulos, and S. G. Johnson, "Meep: A flexible free-software package for electromagnetic simulations by the FDTD method," *Computer Physics Communications*, vol. 181, no. 3, pp. 687–702, 2010.
- [13] P. Allison and et al, "Low-threshold ultrahigh-energy neutrino search with the askaryan radio array," *Phys. Rev. D*, vol. 105, p. 122006, Jun 2022.
- [14] Anker, A, et al, "Probing the angular and polarization reconstruction of the ARIANNA detector at the South Pole," *Journal of Instrumentation*, vol. 15, no. 09, pp. P09039–P09039, 2020.
- [15] M. Estrada, "Creating pathways of kindness and inclusion in stem education." Inclusivity in Introductory STEM Courses, 2022.
- [16] C. Singh, "Promoting equity in science learning." Inclusivity in Introductory STEM Courses, 2022.

- [17] C. Freeman, A. Kittredge, H. Wilson, and B. Pajak, "The duolingo method for app-based teaching and learning," tech. rep., Duolingo Research Report, 2023.
- [18] D. Shin and J. Shim, "A systematic review on data mining for mathematics and science education," *International Journal of Science and Mathematics Education*, pp. 1–21, 2020.
- [19] C. Cooper and P. Pearson, "A genetically optimized predictive system for success in general chemistry using a diagnostic algebra test," *Journal of Science Education and Technology*, vol. 21, no. 1, 2011.
- [20] J. Grossman, Z. Lin, H. Sheng, J. Wei, J. Williams, and S. Goel, "Mathbot: Transforming online resources for learning math into conversational interactions," *Association for the Advancement of Artificial Intelligence (www.aaai.org)*, 2019.
- [21] H. Lee and "et al", "Automated text scoring and real-time adjustable feedback: Supporting revision of scientific arguments involving uncertainty," *Science Education Journal*, vol. 103, no. 3, 2019.
- [22] J. Ghimire, F. D. Diba, J.-H. Kim, and D.-Y. Choi, "Vivaldi Antenna Arrays Feed by Frequency-Independent Phase Shifter for High Directivity and Gain Used in Microwave Sensing and Communication Applications," *Sensors (Basel, Switzerland)*, vol. 21, no. 18, p. 6091, 2021.
- [23] F. Cui, G. Dong, Y. Chen, C. Wang, D. Teng, and R. Wang, "Numerical modeling and data signal analysis of GPR array based on dual-field domain-decomposition time-domain finite element method," *Journal of Applied Geophysics*, vol. 208, p. 104876, 2023.
- [24] R. Mailloux, *The Phased Array Handbook*, 3rd ed. Boston: Artech House, 2017.
- [25] "Xfdtd 3d electromagnetic simulation software." <https://www.remcom.com>. Accessed: 2023-05-23.
- [26] "Ansys hfss." <https://www.ansys.com>. Accessed: 2023-05-23.
- [27] O. Yurduseven, P. Flowers, S. Ye, D. L. Marks, J. N. Gollub, T. Fromenteze, B. J. Wiley, and D. R. Smith, "Computational microwave imaging using 3D printed conductive polymer frequency-diverse metasurface antennas," *IET Microwaves, Antennas & Propagation*, vol. 11, no. 14, pp. 1962–1969, 2017.
- [28] K. Yee, "Numerical solution of initial boundary value problems involving maxwell's equations in isotropic media," *IEEE Transactions on Antennas and Propagation*, vol. 14, no. 3, pp. 302–307, 1966.
- [29] A. Hammond, "High-performance topology optimization for photonics inverse design." MeepCon 2022, 2022.
- [30] The IceCube Collaboration, "Evidence for High-Energy Extraterrestrial Neutrinos at the IceCube Detector," *Science*, vol. 342, no. 6161, pp. 1242856–1242856, 2013.
- [31] M. Ackermann et al, "Astrophysics Uniquely Enabled by Observations of High-Energy Cosmic Neutrinos," 2019.
- [32] M. Ackermann et al, "Fundamental Physics with High-Energy Cosmic Neutrinos," 2019.
- [33] M. Ahlers, L. Anchordoqui, M. Gonzalez-Garcia, F. Halzen, and S. Sarkar, "GZK neutrinos after the Fermi-LAT diffuse photon flux measurement," *Astroparticle Physics*, vol. 34, no. 2, pp. 106–115, 2010.
- [34] K. Kotera, D. Allard, and A. Olinto, "Cosmogenic neutrinos: parameter space and detectability from PeV to ZeV," *Journal of Cosmology and Astroparticle Physics*, vol. 2010, no. 10, p. 013, 2010.
- [35] The IceCube Collaboration, "Differential limit on the extremely-high-energy cosmic neutrino flux in the presence of astrophysical background from nine years of IceCube data," *Physical Review D*, vol. 98, no. 6, p. 062003, 2018.
- [36] The ARIANNA Collaboration, "A search for cosmogenic neutrinos with the ARIANNA test bed using 4.5 years of data," *Journal of Cosmology and Astroparticle Physics*, vol. 2020, no. 03, pp. 053–053, 2020.
- [37] P. Allison, S. Archambault, J. J. Beatty, M. Beheler-Amass, D. Z. Besson, M. Beydler, C. C. Chen, C. H. Chen, P. Chen, B. A. Clark, W. Clay, A. Connolly, L. Cremonesi, J. Davies, S. d. Kockere, K. D. d. Vries, C. Deaconu, M. A. DuVernois, E. Friedman, R. Gaior, J. Hanson, K. Hanson, K. D. Hoffman, B. Hokanson-Fasig, E. Hong, S. Y. Hsu, L. Hu, J. J. Huang, M. H. Huang, K. Hughes, A. Ishihara, A. Karle, J. L. Kelley, R. Khandelwal, K. C. Kim, M. C. Kim, I. Kravchenko, K. Kurusu, H. Landsman, U. A. Latif, A. Laundrie, C. J. Li, T. C. Liu, M. Y. Lu, B. Madison, K. Mase, T. Meures, J. Nam, R. J. Nichol, G. Nir, A. Novikov, A. Nozdrina, E. Oberla, A. O'Murchadha, J. Osborn, Y. Pan, C. Pfendner, J. Roth, P. Sandstrom, D. Seckel, Y. S. Shiao, A. Shultz, D. Smith, J. Torres, J. Touart, N. v. Eijndhoven, G. S. Varner, A. G. Vieregg, M. Z. Wang, S. H. Wang, S. A. Wissel, S. Yoshida, R. Young, and A. Collaboration, "Constraints on the diffuse flux of ultrahigh energy neutrinos from four years of Askaryan Radio Array data in two stations," *Physical Review D*, vol. 102, no. 4, p. 043021, 2020.
- [38] G. Askaryan, "Cherenkov Radiation and Transition Radiation from Electromagnetic Waves," *Soviet Physics JETP*, vol. 15, no. 5, 1962.
- [39] E. Zas, F. Halzen, and T. Stanev, "Electromagnetic pulses from high-energy showers: Implications for neutrino detection," *Physical Review D*, vol. 45, no. 1, p. 362, 1992.

- [40] J. C. Hanson, S. W. Barwick, E. C. Berg, D. Z. Besson, T. J. Duffin, S. R. Klein, S. A. Kleinfelder, C. Reed, M. Roumi, T. Stezelberger, J. Tatar, J. A. Walker, and L. Zou, "Radar absorption, basal reflection, thickness and polarization measurements from the Ross Ice Shelf, Antarctica," *Journal of Glaciology*, vol. 61, no. 227, pp. 438–446, 2015.
- [41] J. Avva, J. Kovac, C. Miki, D. Saltzberg, and A. Vieregg, "An in situ measurement of the radio-frequency attenuation in ice at Summit Station, Greenland," *Journal of Glaciology*, 2014.
- [42] P. Allison, J. Auffenberg, R. Bard, J. Beatty, D. Besson, S. Böser, C. Chen, P. Chen, A. Connolly, and J. Davies, "Design and initial performance of the Askaryan Radio Array prototype EeV neutrino detector at the South Pole," *Astroparticle Physics*, vol. 35, no. 7, pp. 457–477, 2012.
- [43] I. Kravchenko et al, "Updated results from the RICE experiment and future prospects for ultra-high energy neutrino detection at the south pole," *Physical Review D*, vol. 85, no. 6, p. 062004, 2012.
- [44] The ANITA Collaboration, "Constraints on the ultrahigh-energy cosmic neutrino flux from the fourth flight of ANITA," *Physical Review D*, vol. 99, no. 12, p. 122001, 2019.
- [45] D. Saltzberg, P. Gorham, D. Walz, C. Field, R. Iverson, A. Odian, G. Resch, P. Schoessow, and D. Williams, "Observation of the Askaryan effect: coherent microwave Cherenkov emission from charge asymmetry in high-energy particle cascades," *Physical review letters*, vol. 86, no. 13, pp. 2802–5, 2001.
- [46] P. Miocinovic, R. Field, P. Gorham, E. Guilliam, R. Milincic, D. Saltzberg, D. Walz, and D. Williams, "Time-domain measurement of broadband coherent Cherenkov radiation," *Physical Review D*, vol. 74, no. 4, p. 043002, 2006.
- [47] P. W. Gorham, S. W. Barwick, J. J. Beatty, D. Z. Besson, W. R. Binns, C. Chen, P. Chen, J. M. Clem, A. Connolly, P. F. Dowkontt, M. A. DuVernois, R. C. Field, D. Goldstein, A. Goodhue, C. Hast, C. L. Hebert, S. Hoover, M. H. Israel, J. Kowalski, J. G. Learned, K. M. Liewer, J. T. Link, E. Lusczek, S. Matsuno, B. Mercurio, C. Miki, P. Miočinović, J. Nam, C. J. Naudet, J. Ng, R. Nichol, K. Palladino, K. Reil, A. Romero-Wolf, M. Rosen, L. Ruckman, D. Saltzberg, D. Seckel, G. S. Varner, D. Walz, and F. Wu, "Observations of the askaryan effect in ice," *Phys. Rev. Lett.*, vol. 99, p. 171101, Oct 2007.
- [48] J. C. Hanson and R. Hartig, "Complex analysis of askaryan radiation: A fully analytic model in the time domain," *Phys. Rev. D*, vol. 105, p. 123019, Jun 2022.
- [49] K. Dookayka, *Characterizing the Search for Ultra-High Energy Neutrinos with the ARIANNA Detector* DISSERTATION. PhD thesis, University of California, Irvine, 2011.
- [50] The ARA Collaboration, "First constraints on the ultra-high energy neutrino flux from a prototype station of the askaryan radio array," *Astroparticle Physics*, vol. 70, pp. 62–80, 2015.
- [51] C. Glaser, D. García-Fernández, A. Nelles, J. Alvarez-Muñiz, S. W. Barwick, D. Z. Besson, B. A. Clark, A. Connolly, C. Deaconu, K. D. d. Vries, J. C. Hanson, B. Hokanson-Fasig, R. Lahmann, U. Latif, S. A. Kleinfelder, C. Persichilli, Y. Pan, C. Pfendner, I. Plaisier, D. Seckel, J. Torres, S. Toscano, N. v. Eijndhoven, A. Vieregg, C. Welling, T. Winchen, and S. A. Wissel, "NuRadioMC: simulating the radio emission of neutrinos from interaction to detector," *The European Physical Journal C*, vol. 80, no. 2, p. 77, 2020.
- [52] C. Glaser, A. Nelles, I. Plaisier, C. Welling, S. W. Barwick, D. García-Fernández, G. Gaswint, R. Lahmann, and C. Persichilli, "NuRadioReco: a reconstruction framework for radio neutrino detectors," *The European Physical Journal C*, vol. 79, no. 6, p. 464, 2019.
- [53] C. Welling, P. Frank, T. A. Enßlin, and A. Nelles, "Reconstructing non-repeating radio pulses with Information Field Theory," *arXiv*, 2021.
- [54] S. Barwick, E. Berg, D. Besson, T. Duffin, J. Hanson, S. Klein, S. Kleinfelder, M. Piasecki, K. Ratzlaff, C. Reed, M. Roumi, T. Stezelberger, J. Tatar, J. Walker, R. Young, and L. Zou, "Time-domain response of the ARIANNA detector," *Astroparticle Physics*, vol. 62, pp. 139–151, 2015.
- [55] S. W. Barwick, E. C. Berg, D. Z. Besson, G. Gaswint, C. Glaser, A. Hallgren, J. C. Hanson, S. R. Klein, S. Kleinfelder, L. Köpke, I. Kravchenko, R. Lahmann, U. Latif, J. Nam, A. Nelles, C. Persichilli, P. Sandstrom, J. Tatar, and E. Unger, "Observation of classically 'forbidden' electromagnetic wave propagation and implications for neutrino detection," *Journal of Cosmology and Astroparticle Physics*, vol. 2018, no. 07, pp. 055–055, 2018.
- [56] The ARA Collaboration, "Measurement of the real dielectric permittivity ϵ_r of glacial ice," *Astroparticle Physics*, vol. 108, pp. 63–73, 2019.
- [57] S. Barwick, E. Berg, D. Besson, G. Binder, W. Binns, D. Boersma, R. Bose, D. Braun, J. Buckley, V. Bugaev, S. Buitink, K. Dookayka, P. Dowkontt, T. Duffin, S. Euler, L. Gerhardt, L. Gustafsson, A. Hallgren, J. Hanson, M. Israel, J. Kiryluk, S. Klein, S. Kleinfelder, H. Niederhausen, M. Olevitch, C. Persichelli, K. Ratzlaff, B. Rauch, C. Reed, M. Roumi, A. Samanta, G. Simburger, T. Stezelberger, J. Tatar, U. Uggerhoj, J. Walker, G. Yodh, and R. Young, "A first search for cosmogenic neutrinos with the ARIANNA Hexagonal Radio Array," *Astroparticle Physics*, vol. 70, pp. 12–26, 2015.

- [58] S. Barwick, D. Besson, A. Burgman, E. Chiem, A. Hallgren, J. Hanson, S. Klein, S. Kleinfelder, A. Nelles, C. Persichilli, S. Phillips, T. Prakash, C. Reed, S. Shively, J. Tatar, E. Unger, J. Walker, and G. Yodh, "Radio detection of air showers with the arianna experiment on the ross ice shelf," *Astroparticle Physics*, 2016.
- [59] J A Aguilar et al, "Design and Sensitivity of the Radio Neutrino Observatory in Greenland (RNO-G)," *arXiv*, 2020.
- [60] S. Barwick, E. Berg, D. Besson, G. Gaswint, C. Glaser, A. Hallgren, J. Hanson, S. Klein, S. Kleinfelder, L. Köpke, I. Kravchenko, R. Lahmann, U. Latif, J. Nam, A. Nelles, C. Persichilli, P. Sandstrom, J. Tatar, and E. Unger, "Observation of classically 'forbidden' electromagnetic wave propagation and implications for neutrino detection.," *Journal of Cosmology and Astroparticle Physics*, vol. 2018, no. 07, p. 055, 2018.
- [61] C. Deaconu, A. G. Vieregg, S. A. Wissel, J. Bowen, S. Chipman, A. Gupta, C. Miki, R. J. Nichol, and D. Saltzberg, "Measurements and modeling of near-surface radio propagation in glacial ice and implications for neutrino experiments," *Phys. Rev. D*, vol. 98, p. 043010, Aug 2018.
- [62] S. Barwick, E. Berg, D. Besson, T. Duffin, J. Hanson, S. Klein, S. Kleinfelder, K. Ratzlaff, C. Reed, M. Roumi, T. Stezelberger, J. Tatar, J. Walker, R. Young, and L. Zou, "Design and Performance of the ARIANNA HRA-3 Neutrino Detector Systems," *IEEE Transactions on Nuclear Science*, vol. 62, no. 5, pp. 2202–2215, 2015.
- [63] S. W. Barwick *et al.*, "A First Search for Cosmogenic Neutrinos with the ARIANNA Hexagonal Radio Array," *Astropart. Phys.*, vol. 70, pp. 12–26, 2015.
- [64] J. Hanson, "Broadband RF Phased Array Design for UHE neutrino detection," *Proceedings of 37th International Cosmic Ray Conference — PoS(ICRC2021)*, p. 1217, 2021.
- [65] S. Barwick, D. Besson, P. Gorham, and D. Saltzberg, "South polar in situ radio-frequency ice attenuation," *Journal of Glaciology*, vol. 51, no. 173, p. 231–238, 2005.
- [66] M. Stockham, J. Macy, and D. Besson, "Radio frequency ice dielectric permittivity measurements using CReSIS data," *Radio Science*, vol. 51, no. 3, pp. 194–212, 2016.
- [67] X. Shi, F. Park, L. Wang, J. Xin, and Y. Qi, "Parallelization of a color-entropy preprocessed chan–vese model for face contour detection on multi-core cpu and gpu," *Parallel Computing*, vol. 49, pp. 28–49, 2015.
- [68] K. Bui, F. Park, Y. Lou, and J. Xin, "A weighted difference of anisotropic and isotropic total variation for relaxed mumford–shah color and multiphase image segmentation," *SIAM Journal on Imaging Sciences*, vol. 14, no. 3, pp. 1078–1113, 2021.
- [69] A. Majumder, "Ultracompact nanophotonic devices and diffractive structures for imaging." MeepCon 2022, 2022.
- [70] A. Oskooi, "Tutorial #2: Diffraction efficiency of binary gratings." MeepCon 2022, 2022.
- [71] A. Hammond, "Tutorial #3: Inverse design of a power splitter for silicon photonics." MeepCon 2022, 2022.
- [72] K. Staats, "Genetic programming applied to RFI mitigation in radio astronomy," Master's thesis, University of Cape Town, South Africa, Dec. 2016.
- [73] S. Ventura, *Genetic Programming - New Approaches and Successful Applications*. InTech, 2012.